Gigahertz-Peaked Spectrum (GPS) Galaxies and Quasars

M. G. Mingaliev[1,2]*, Yu. V. Sotnikova[1]**, T. V. Mufakharov[1]***, A. K. Erkenov[1]****, and R. Yu. Udovitskiy[1]*****

[1]*Special Astrophysical Observatory, Russian Academy of Sciences, Nizhnii Arkhyz, 369167 Russia*
[2]*Kazan (Volga Region) Federal University, Kazan, 420008 Russia*
Received May 22, 2013; in final form, June 18, 2013

Abstract—The results of a comprehensive analysis of continuous radio spectra of a sample of Gigahertz-Peaked Spectrum (GPS) sources are reported. The sources are selected from a flux-density-complete sample ($S_\nu \geq 200$ mJy at 4.8 or 5 GHz) using multifrequency measurements of the RATAN-600 radio telescope and data from the CATS astrophysical catalogs support system. The analysis revealed a very small number (1–2%) of "classical" GPS objects, which is significantly less than the expected fraction of 10%. GPS galaxies are found to have narrower and steeper radio spectra than quasars. The low-frequency part of the spectrum is seen to become steeper with increasing redshift. Galaxies and quasars at the same z have comparable angular sizes, whereas their luminosities may differ by one order of magnitude. At large redshifts there is a deficit of objects with low (several GHZ) peak frequencies. The number of GPS galaxies decreases sharply with redshift, and most of them are found at z between 0.01 and 1.81. GPS quasars are found at large redshifts, from 0.11 to 3.99. A quarter of the sample consists of blazars whose spectra may temporarily have a convex shape when the object is in active state.

1. INTRODUCTION

GPS (Gigahertz Peaked-Spectrum) galaxies and quasars are powerful radio sources with a convex radio spectrum that peaks between 0.5 and several tens of GHz (observer's frame) [1–4]. GPS objects are characterized by a small size (less than 1 kpc) and low variability amplitude. Because of their small angular sizes the structure of these sources can be resolved only partially even in VLBI observations. For a detailed description of the properties of GPS objects see [3, 4]. Most of our knowledge about GPS objects was obtained statistically. The samples studied often include quasars with a peak in the radio spectrum [5, 6] (hereafter referred to as FSRQ—Flat Spectrum Radio Quasars). The conclusions so far obtained are influenced by selection effects due to natural restrictions on increasing the sample size simultaneously with expanding the frequency interval. Analysis of the nature of GPS sources are further complicated by the lack of homogeneous samples

covering a wide frequency range and allowing their intrinsic properties to be determined.

GPS galaxies are characterized by low redshifts ($0.1 \leq z \leq 1$) and they have a rather low radio variability compared to the GPS quasars [7–9]. Furthermore, GPS galaxies have spectra peaking at lower frequencies [9] and it is more common for them to have a symmetric structure when observed with VLBI. Quasars of this type usually exhibit a more complex or a core–jet type structure [10, 11].

The currently favored view is that the galaxy-type GPS sources are intrinsically small due to their young age [3, 12–15]. These objects are believed to be the progenitors of extended radio sources, as corroborated by kinematic and spectral studies, which yield ages on the order of 10^3–10^5 yr. Another scenario explains the small linear sizes of GPS galaxies by their dense environment [3, 16]: such sources are not young, but remain small because of the external pressure preventing their expansion. Small linear sizes of GPS quasars are sometimes explained by projection effects [17].

The results of simultaneous measurements in many parts of the electromagnetic spectrum are used extensively in recent studies. This brought about the emergence of new techniques and approaches to

*E-mail: `marat@sao.ru`
**E-mail: `sjv@sao.ru`
***E-mail: `timmy23@mail.ru`
****E-mail: `artur@sao.ru`
*****E-mail: `nemiroff@sao.ru`

AGN studies. Bai and Lee [18] suggested, based on X-ray measurements, that GPS quasars are blazars in a dense gas and dust environment. That is why, although their jets are oriented at a small angle to the line of sight, these sources do not exhibit blazar properties (flat radio spectrum and radio-emission variations with amplitudes up to several tens of percent). The nature of GPS quasars is not yet entirely understood. Most of the conclusions and hypotheses were based on small samples, detailed studies of several objects, or samples contaminated by objects of other types because of classification errors.

Studies of GPS objects usually involve the analysis of the following parameters of their radio spectra: peak frequency in the observer's (ν_{obs}) or rest ($\nu_{\mathrm{intrinsic}}$) frame; spectral indices below (α_{below}) and above (α_{above}) the peak frequency, which characterize the optically thick and thin emission region, respectively, and the full width at half maximum FWHM of the fitted spectra in frequency decades [3]. In some cases constraints are imposed on the peak frequency for GPS objects: $0.5 \leq \nu_{\mathrm{obs}} \leq 10$ GHz. Objects with peak frequencies below 0.5 or above 10 GHz belong to the CSS (Compact Steep Spectrum) [19–21] and HFP (High-Frequency Peakers) classes [22], respectively. Researchers often use the notion of a "classical" or "canonical" spectrum of a GPS object [5]. These are spectra whose form is most similar to that of the theoretical spectra corresponding to synchrotron emission of a homogeneous object with self-absorption at low frequencies [23]. For example, Vries et al. [5] adopt as the "canonical" GPS spectrum the radio spectrum with α_{below} and α_{above} equal to $+0.5$ and -0.7, respectively. O'Dea et al. [3] consider the spectral width FWHM ≤ 1.2 to be one of the parameters of the "classical" GPS.

In 2006–2011 systematic monitoring of 122 candidate GPS was carried out at the RATAN-600 radio telescope. As a result, simultaneous broadband radio spectra (at 1.1, 2.3, 4.8, 7.7, 11.2, and 21.7 GHz) and some preliminary results [24–26] have been obtained. Only 25% of the objects of this sample were found to have the properties of a "classical" GPS [5]. High-frequency spectral indices and widths of radio spectra differ statistically for GPS galaxies and quasars [26]. It is possible that different physical mechanisms or ambient conditions, rather than only the jet position angle, play the crucial role in the formation of the spectra of GPS galaxies and quasars [17, 27]. We expanded the sample of GPS objects to perform a further comparison with our results obtained in 2006–2011. To this end, we selected GPS candidates from a flux-density complete sample ($S_\nu \geq 200$ mJy at 4.8 or 5 GHz) based on the CATS database [28]. In total, the sample contains about 5000 sources. We selected 467 objects with convex radio spectra, which we considered to be GPS candidates. We adopt the spectral parameters for the GPS candidates observed at the RATAN-600 during the 2006–2011 period from our previous paper [26].

In this paper we report the results of a comprehensive study of a sample of GPS candidates, which includes bright objects of both the Northern and Southern hemisphere. The weak point of this study is the use of inhomogeneous observational data obtained with different instruments and at different epochs. Some of the bright objects were observed systematically at several frequencies within the framework of AGN monitoring programs, whereas some objects are poorly represented at low and high radio frequencies. We study various observational parameters of the objects in order to try to separate GPS galaxies and quasars.

2. SAMPLE PROPERTIES

We selected objects with convex radio spectra from a flux-density complete sample: $S_\nu \geq 200$ mJy at 4.8/5 GHz (we define the spectral index α such that $S \sim \nu^\alpha$). As a result, we selected 467 GPS candidates by spectral type, with redshift data available for 249 of these objects. The sample contains 118 galaxies, 187 quasars, and 162 sources without optical counterparts. We list the objects in Table 1. Notes for the columns:

(1) source name in J2000 coordinates;

(2, 3) the optical counterpart and redshift (NASA/IPAC Extragalactic Database);

(4) the peak frequency ν_{obs} in the observer's frame, in GHz;

(5) the spectral flux density at the peak frequency, in Jy;

(6) value of FWHM in frequency decades;

(7, 8) the spectral indices below (α_{below}) and above (α_{above}) the peak frequency;

(9) the angular size of the emitting region in mas;

(10) the blazar type according to the BZCAT catalog [29]: FSRQs—flat spectrum radio quasars, BL Lac—BL Lac-type objects, BL Lac cand.—candidate BL Lac-type objects, Blz.un.t—unknown-type blazars;

(11) the morphological type based on VLBI data;

(12) the flux density variability index in percent: >25 and <25 for higher and lower than 25% variability indices, respectively, "lack" for objects with insufficient experimental data for variability index estimates;

Table 1. List of objects and the computed parameters of the radio spectra

Name	Type	z	ν_{obs}, GHz	$f_{5\,GHz}$, Jy	FWHM	$\alpha_{below} \pm \sigma$	$\alpha_{above} \pm \sigma$	θ, mas	Type of blazar	Morph.	Vars, %	Remark
(1)	(2)	(3)	(4)	(5)	(6)	(7)	(8)	(9)	(10)	(11)	(12)	(13)
000020−322101	Q	1.28	2.56	0.54	1.4	$+0.43 \pm 0.012$	-0.70 ± 0.014	0.38	FSRQ		lack	
000053+405402	G		0.35	1.84	2.0	$+0.36 \pm 0.009$	-0.56 ± 0.002				<25	
000316−194150	G		1.97	0.27	1.5	$+0.44 \pm 0.017$	-0.71 ± 0.007				lack	
000319+212944	G	0.40	3.33	0.21	1.1	$+0.37 \pm 0.015$	-0.90 ± 0.009	0.15	FSRQ	cso	<25	g*
000346+480703			1.91	0.28	1.3	$+1.04 \pm 0.027$	-1.45 ± 0.018				lack	g
000520+052410	Q	1.89	4.13	0.26	1.3	$+0.51 \pm 0.006$	-0.82 ± 0.005	0.15	FSRQ	cso	<25	g
000800−233918	Q	1.41	2.90	0.56	1.4	$+0.55 \pm 0.005$	-0.83 ± 0.006	0.33	FSRQ		lack	
001004−685129			1.89	0.28	1.4	$+0.09 \pm 0.012$	-1.21 ± 0.009				lack	
001052−415310	G		0.46	6.84	1.6	$+0.13 \pm 0.006$	-1.14 ± 0.003	10.94			<25	
001534−180726			0.98	0.37	1.8	$+0.24 \pm 0.002$	-0.52 ± 0.007				lack	
002127+731241	G	0.82	0.92	0.72	1.6	$+0.31 \pm 0.005$	-0.89 ± 0.011	1.45			<25	
002225+001456	G	0.31	0.61	3.12	1.7	$+0.36 \pm 0.008$	-0.87 ± 0.002	4.63		cd	<25	
002442−420203	Q	0.94	1.94	2.72	1.3	$+0.97 \pm 0.003$	-1.32 ± 0.004	1.14		cso	<25	g
002914+345632	G	0.52	1.35	1.76	1.7	$+0.56 \pm 0.016$	-0.43 ± 0.001	1.36		cd	<25	
003714−214525	Q	2.51	5.40	0.24	1.4	$+1.07 \pm 0.010$	-0.27 ± 0.003				lack	
003732+080813	G	1.80	5.15	0.27	1.0	$+0.52 \pm 0.013$	-0.70 ± 0.008	0.12			<25	g
003820−032959	Q	1.86	3.44	0.32	1.3	$+0.66 \pm 0.004$	-1.13 ± 0.012	0.21	FSRQ		<25	g
003830−212004	G	0.34	0.32	1.10	2.3	$+0.36 \pm 0.008$	-0.52 ± 0.005				<25	
004858+064006	Q	3.58	2.69	0.26	1.2	$+0.31 \pm 0.014$	-1.32 ± 0.013				lack	g
005509−412502	Q	2.49	3.25	0.23	1.2	$+0.70 \pm 0.003$	-0.95 ± 0.006	0.21			lack	g
005855−521927	Q		5.00	0.23	1.4	$+1.00 \pm 0.013$	-0.28 ± 0.007		BL Lac		lack	

(13) objects with classical GPS properties ("g"), the asterisk ("g*") denotes the objects identified as GPS in [2].

We adopt the morphological type data from [3, 10, 30−38], where:

cd = compact double structure;

cso = compact symmetric structure;

ct = compact triple structure;

cx = complex structure;

cj = core−jet structure;

c = core dominated structure;

unres = unresolved.

The full text of Table 1 is available at the Strasbourg astronomical Data Center (CDS).

Information about radio morphology is known only for a small part of the sample, however, the galaxies usually have a compact symmetric or complex structure (cso and cx), and quasars, the core/core−jet (c/cj) or unresolved (un) structure. This means that the powerful radio emission of most of the GPS galaxies is their intrinsic property and not a result of Doppler boosting radiation.

Figure 1 shows the relation $z−\nu_{intrinsic}$ between redshift and the intrinsic peak frequency for sample objects with observed peak frequencies (see Section 5) $0.5 \leq \nu_{obs} \leq 10$ GHz (see Table 1). The intrinsic peak frequency range grows with a $(1 + z)$ factor. The dashed line in Fig. 1 shows the peak frequency evolution.
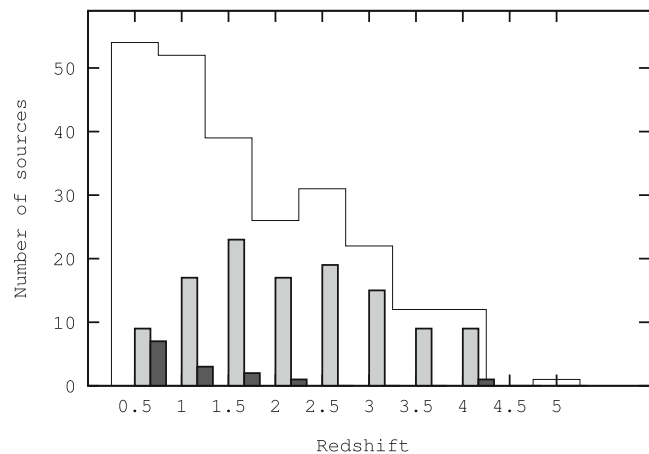
3. REDSHIFT DISTRIBUTION

We adopt the redshifts of sample sources from the NED/IPAC database. We found them to be available for 53% of the objects. The redshift distribution is presented in Fig. 2.

The Roma-BZCAT catalog [29] contains some sources from our sample (132). This catalog is an extensive list of blazars based on the results of multifrequency surveys and a careful examination of published studies, and contains 3149 objects to date. The inclusion of GPS candidates in the blazar catalog is due to the problem of identifying their nature, which still remains a topic of extensive debate. According to the generally adopted classification, sources whose spectra peak at high frequencies (several tens of GHz) are the so-called High-Frequency Peakers, or HFP objects [22]. HFP and GPS sources are a mix of galaxies and quasars including BL Lac type objects. Multifrequency observations revealed that some of these sources are indeed variable and that their spectral shapes vary from convex to flat [6, 26].
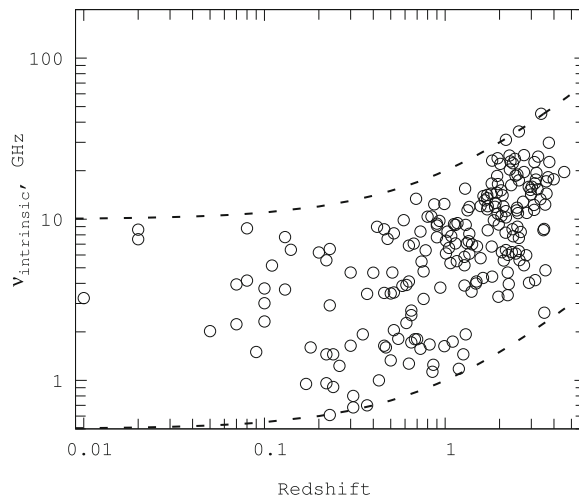

Fig. 1. Variation of the intrinsic peak frequency $\nu_{intrinsic}$ with redshift z for objects of the entire sample with observed peak frequencies $0.5 \leq \nu_{obs} \leq 10$ GHz. The dashed line shows the evolution for the 0.5 and 10 GHz frequencies as a function of redshift.

Fig. 2. Redshift distribution for the entire sample (the thin line); the black bars show the distribution of redshifts for BL Lac type objects and blazars of unknown type according to the classification of Massaro et al. [29] (14 sources), and the gray bars show the redshift distribution for FSRQ objects (118 sources).

Such variations led the authors of the above catalog to suggest the existence of a link between GPS/HFP and blazars. Experimental data for most of the radio sources are insufficient in terms of frequency and time coverage. That is why the GPS objects exhibiting blazar properties [29] were included in the Roma-BZCAT catalog.

Figure 2 represents separate redshift distribution histograms for the FSRQ and BL Lac type objects. As is evident from the figure, our sample is contam-
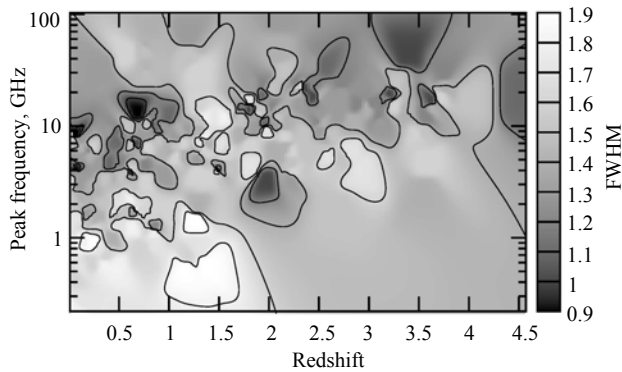
Fig. 3. The redshift−peak frequency−radio-spectrum width (z−$\nu_{\mathrm{intrinsic}}$−FWHM) relation for all the objects of the sample whose spectra peak at radio frequencies. The peak frequency is in the rest frame of the source. Most of the radio sources with narrow spectra (FWHM ≤ 1.1) are located in the redshift domains $z < 1$ and $z > 3$.

inated by a large fraction of blazars, which include BL Lac and candidate BL Lac type objects at small redshifts (three sources), FSRQ type objects at larger redshifts (118 sources), and 11 blazars of unknown type.

Figure 3 shows the redshift−peak frequency−radio-spectrum width (z−$\nu_{\mathrm{intrinsic}}$−FWHM) diagram for all the objects of the sample whose spectra peak at radio frequencies. This relation is characteristic of the distribution of compact objects with relatively uniform synchrotron emission. The relation covers all objects (467), including those caught at the time of activity, when radio emission from a compact nuclear region dominates, and the radio spectrum becomes temporarily convex. It can be clearly seen in the figure that the radio sources with the narrowest spectra (FWHM ≤ 1.1) are located at the redshift domains $z < 1$ and $z > 3$.

Figure 4 shows the redshift−peak frequency relations for galaxies and quasars, and Fig. 5 shows the corresponding relations for FSRQ, BL Lac type objects, blazars of unknown type, and objects that exhibit no blazar properties. The characteristic feature of blazars is variable radio emission and therefore the sample contains a substantial number of objects with temporarily convex radio spectra. The similarity of Figs. 4 and 5 is immediately apparent: the redshift distribution of the objects is such that most of the quasars coincide with FSRQ objects of the BZCAT catalog, and most of the galaxies, with objects exhibiting no blazar properties. It is therefore possible that a large fraction of the sample quasars might not be the genuine GPS sources.

4. RADIO VARIABILITY

We use the `spg` module of the `FADPS` [39] data processing system to compute the parameters of the radio spectra of the objects studied. We compute the spectral indices α_{above} and α_{below} by fitting linear relations to the portions of the radio spectrum above and below the peak frequency, respectively. For simplicity, we compute the peak frequency and spectrum width by fitting the spectrum to a parabola. To quantify the flux-density variability, we compute the variability index by the following formula adopted from [40]:

$$\mathrm{Var}_S = \frac{(S_{\max} - \sigma_i)_{\max} - (S_i + \sigma_i)_{\min}}{(S_i - \sigma_i)_{\max} + (S_i + \sigma_i)_{\min}}, \quad (1)$$

where S_i and σ_i are the flux density and its error at the i-th observing epoch, and max and min are the indices corresponding to the maximum and minimum flux density, respectively. The observed flux-density data at various frequencies found in the available catalogs are inhomogeneous. In order to estimate the radio variability, we calculate the variability index at the frequencies where observations were repeatedly made: 960, 1400, 2700, 4800, 5000, 7700, 11 200, 15 000, 31 400, and 95 600 MHz. Almost half of the objects have variability amplitudes no greater than 25%. For about 42% of the sources the variability amplitude cannot be estimated because of insufficient observational data. The maximum variability amplitude (53%) is observed for J 1558−1410 at 15 GHz.

5. GPS CANDIDATES

We use the following criteria adopted in [3, 5, 41] to select GPS candidates:

− spectral indices $\alpha_{\mathrm{below}} \geq +0.5$ and $\alpha_{\mathrm{above}} \leq -0.7$;

− FWHM ≤ 1.2 frequency decades;

− peak frequency $\nu_{\mathrm{obs}} \geq 500$ MHz;

− variability index $\mathrm{Var}_S \leq 25\%$.

The authors of the above studies estimated the spectral indices by the mean radio spectrum normalized to maximum flux. They constructed the normalized radio spectrum for an individual object by scaling both the peak frequency and flux density to unity [5]. The normalized radio spectra of GPS candidates were then averaged. The additional parameter that allows distinguishing between GPS and CSS (Compact Steep Spectrum) objects [19−21] is the observed peak frequency, which is below 500 MHz for CSS objects. The variability index constraint serves to partially exclude variable quasars with flat spectra [6, 26]. In this paper we pay special attention to the flux-density variability at the most commonly used frequencies: objects with variability amplitudes greater
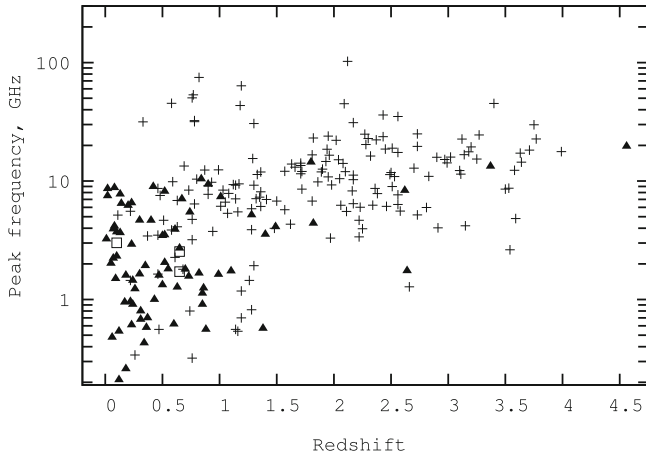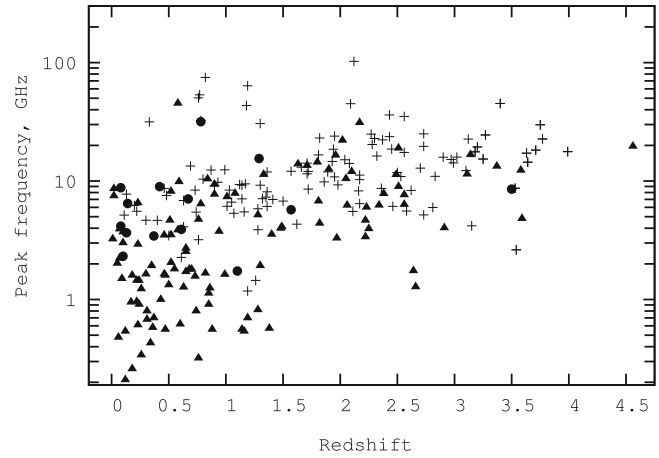
Fig. 4. Redshift−peak frequency ν_{obs} relations for galaxies (triangles), quasars (crosses), and unidentified radio sources (squares) among the sample objects with known z.


Fig. 5. Redshift−peak frequency ν_{obs} relation for FSRQ (crosses), BL Lac type objects and blazars of unknown type (circles), and objects exhibiting no blazar properties (triangles); the relation is plotted for all the objects with known z.

than 25% at more than two frequencies appear to be blazars, quasars with flat spectra, or BL Lac type objects.

Our analysis of the radio spectra of all 467 sources revealed only 44 objects with the properties of a classical GPS. This makes up about 10% of all the sources with a spectral maximum (467) and only about 1% of our entire sample (about 5000 objects). Given the inhomogeneity of the data and the possibility of missing some of the objects because of inaccurately measured parameters, we relaxed the selection criteria and expanded the candidate list by including objects with FWHM ≤ 1.4, and α_{below} and α_{above} of about $+0.5$ and -0.7, respectively. In Table 1 the GPS candidates so selected are marked by letter "g." This is 2% of the total sample (5000 objects). We identified a total of 112 objects with the properties of classical GPS and possible candidates. These include 43 quasars, 18 galaxies, and 48 unidentified objects. The estimates of the parameters of the radio spectra used to select GPS candidates are based on the CATS database or RATAN-600 data (such objects are marked by an asterisk ("g*") in Table 1).

6. PEAK FREQUENCY VS. RADIO LUMINOSITY

There is an obvious deficit of objects in the domain of large redshifts and small $\nu_{\mathrm{intrinsic}}$ on the plot of the redshift dependence of the intrinsic peak frequency (Fig. 1). Distant objects may have unknown redshifts and insufficiently high radio luminosities with their steep radio spectra and low peak frequencies. Such objects should then fill the bottom right part of the $z-\nu_{\mathrm{intrinsic}}$ diagram in Fig. 1. To distinguish
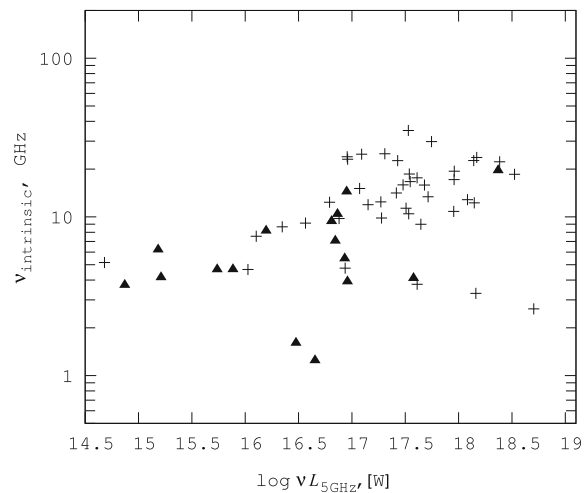
Fig. 6. Intrinsic frequency $\nu_{\mathrm{intrinsic}}$ as a function of radio luminosity for galaxies (triangles) and quasars (crosses).

high and low radio luminosity objects with low peak frequencies, we analyzed the radio luminosity $\log(\nu L_{5\mathrm{GHz}})$−peak frequency $\nu_{\mathrm{intrinsic}}$ relation (Fig. 6). We use standard relations with the adopted cosmological constants $H_0 = 71$ km s^{-1} Mpc^{-1}, $\Omega_m = 0.27$, and $\Omega_\Lambda = 0.73$ to compute the 5 GHz luminosities. In our analysis we use the data for the sample of GPS candidates ("g" in Table 1), which includes 112 sources. Because of the lack of redshift data for some objects, the plot features 17 galaxies and 41 quasars.

The anticorrelation between the peak frequency and angular size (equation (2)) [23, 45, 46] suggests that the deficit of objects in the bottom right corner
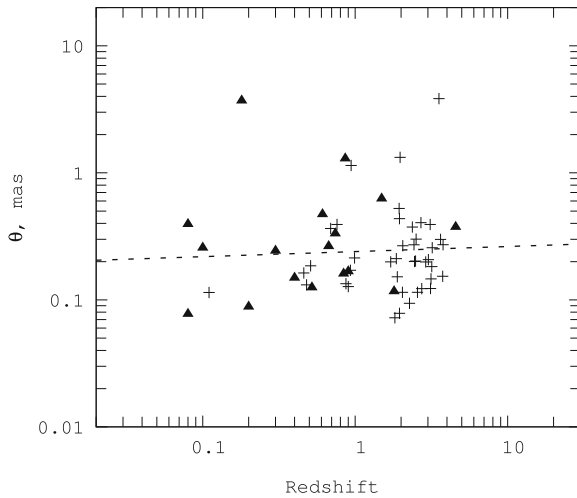
Fig. 7. Angular size of the emitting region vs. the redshift of GPS candidates. Designations are the same as in Fig. 6.

of Fig. 1 means that at large z there are no large self-absorbed synchrotron components. If we assume that free-free absorption might cause the spectrum turnover at low frequencies, we again confirm the presence of high-density matter in circumnuclear regions of young objects. Vries et al. [5] analyzed a sample of 72 GPS candidates and found their sizes to sharply decrease and $\nu_{\mathrm{intrinsic}}$ to increase with increasing radio luminosity (the converse is not true). This results in the deficit of large objects with high radio luminosities at large redshifts.

7. ANGULAR SIZES

GPS sources may consist of several components. Registered emission is the sum of the contributions of all components (if the object does not differ from a point source for the power beam pattern considered). We can infer an upper estimate for the size of the emitting region assuming that synchrotron (and not free-free) absorption is responsible for the formation of the peak in the spectrum of the GPS source. The peak frequency for a self-absorbed radio source with a power-law distribution of electron energies, homogeneous structure, and magnetic field can be computed

Table 2. Parameters of the normalized radio spectrum of GPS galaxies and quasars

Type	α_{below}	α_{above}	FWHM
G	$+1.01 \pm 0.002$	-0.81 ± 0.002	1.4
QSO	$+0.90 \pm 0.002$	-0.59 ± 0.001	1.6

as [23]

$$\nu_{\mathrm{max}} = 8B^{1/5}S_{\mathrm{max}}^{2/5}\theta^{-4/5}(1+z)^{1/5}, \qquad (2)$$

where B is the magnetic field strength in Gauss; S_{max} is the flux density at peak frequency in Jy; θ is the angular size in mas, and ν_{max} is the peak frequency in GHz. We set the magnetic field strength for compact radio sources equal to 100 μG [42] to derive the following formula for the angular size of the source

$$\theta \approx 1.345\frac{\sqrt{S_{\mathrm{max}}}(1+z)^{1/4}}{\nu_{\mathrm{max}}^{5/4}}. \qquad (3)$$

This relation determines the upper limit for the size of the emitting region (that produces the "convex" radio spectrum) and has nothing to do with the physical size of the object. We obtained the dependence of angular size θ on redshift z for the objects with known redshifts from the sample of GPS candidates (Fig. 7). The angular sizes of the selected GPS objects do not exceed 10 mas, which agrees well with the results of VLBI measurements of the sizes of compact objects [43, 44]. On the average, the angular sizes of quasars in our sample are smaller than those of galaxies, but they are of the same order of magnitude for objects of both types at the same z. The anticorrelation between linear size and peak frequency [45, 46] means that more luminous and larger-redshift quasars (see Fig. 4) are more compact, because they have higher rest frame peak frequencies $\nu_{\mathrm{intrinsic}}$ (Fig. 6).

8. NORMALIZED RADIO SPECTRUM

To compare the shapes of the spectra of GPS galaxies and quasars ("g"), we constructed the normalized radio spectra of these objects (Figs. 8 and 9). Normalization to the observed peak frequencies and flux densities allows the radio spectra to be compared to each other [5]. Redshift binning makes apparent the evolutionary effects on the shape of the radio spectrum. Theoretically all the spectra should pass through the same point: $\nu/\nu_{\mathrm{max}} = 1$ and $S(\nu)/S(\nu_{\mathrm{max}}) = 1$. Variations of flux densities observed on different instruments and the approximate determination of the peak (via a parabolic fit) result in a certain scatter of data points at the peak of the normalized spectrum. We model the normalized radio spectrum by two straight lines (in logarithmic scale) that intersect at the maximum (peak). We define the peak as described above in Section 4. Table 2 lists the parameters of the normalized radio spectrum of GPS galaxies and quasars. On the whole, the average radio spectrum of GPS galaxies is steeper at the frequencies above and below the peak. As a result, galaxies have a more narrow average normalized radio spectrum FWHM = 1.4 than quasars FWHM = 1.6.
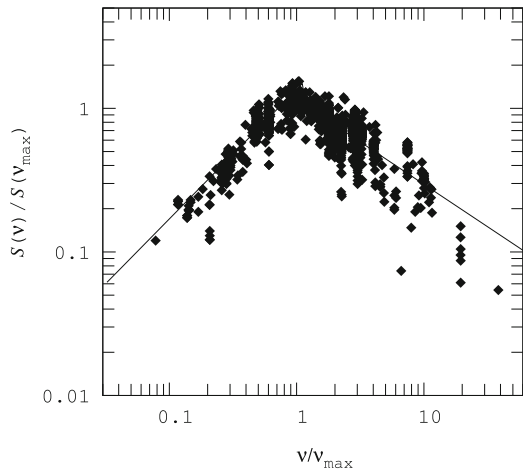
Fig. 8. Normalized radio spectrum of GPS quasars based on our sample of candidate objects (marked as "g" in Table 1). The least squares method yields the following spectral indices: $\alpha_{below} = +0.90 \pm 0.002$ and $\alpha_{above} = -0.59 \pm 0.001$.
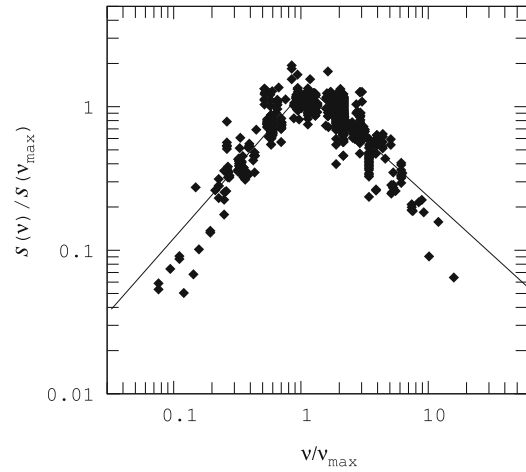
Fig. 9. Normalized radio spectrum of GPS galaxies based on our sample of candidate objects (marked as "g" in Table 1). The least squares method yields the following spectral indices: $\alpha_{below} = +1.01 \pm 0.002$ and $\alpha_{above} = -0.81 \pm 0.002$.

The sample was subdivided into two redshift bins $z = 0-1$ and $1-5$ to find the differences between GPS galaxies and quasars. To reveal the evolutionary effects on the shape of the spectra, we subdivided the GPS candidates into the redshift bins $z = 0-2$ and $2-5$. We present the results in Table 3, from which it is apparent that α_{below} varies by about 0.2 starting from $z = 1$. Note that earlier studies reported finding no statistical differences between the mean α_{below} indices for the subsamples of GPS galaxies and quasars [3, 5, 6]. The spectral index α_{above} varies in the process of evolution and differs by $0.04-0.07$ for the two types of objects. Thus galaxies have, on the average, greater α_{above} indices. The α_{below} index increases in absolute value with z.

9. DISCUSSION

In this study we find about 2% of the sources to be "classical" GPS objects, which is significantly less than the expected 10% [2]. This is due to the fact that major studies of GPS objects [2−5] are based on the results of non-simultaneous observations carried out over a too short time span. Our classification is based on heterogeneous observational data (CATS) and on the results of simultaneous long-term observations made with the RATAN-600 radio telescope. The resulting list of selected candidates includes one third of FSRQs—37 objects, which may prove not to be GPS. Information about their variability remains inconsistent. Long-term monitoring [26] shows that a substantial fraction of GPS objects are variable at radio frequencies (tens of percent), whereas weak variability is a rather rare phenomenon, which is more often found in GPS galaxies and is possibly due to the

lack of observations at different frequencies [6, 25, 47]. In this paper we estimate the variability index Var_S. For a substantial part of the objects it does not measure the real variation of spectral flux density S_ν at all frequencies because of the inhomogeneity of the available observational data.

It is obvious that GPS sources are an inhomogeneous group of objects. Similar properties are observed within subgroups or for single sources. GPS quasars are not as popular as galaxies among the authors of published studies. Currently, GPS quasars are known to have smaller linear sizes (possibly due to the orientation of the jet with respect to the observer), larger redshifts, higher peak frequencies, and stronger variability. Based on his study of a small quasar sample (21 objects), O'Dea [8] found that half of ultra-distant ($z \geq 3$) quasars are GPS type sources and half of GPS quasars are located at large z. Barthel and Miley [48] attribute this to the dense gas and dust medium surrounding the quasars located at large redshifts, which prevents the propagation of radiation through the interstellar medium. The unusually steep radio spectra of GPS quasars compared to those of

Table 3. Spectral parameters for different redshift intervals

Redshift interval	α_{below}	α_{above}	FWHM
0−1	$+0.73 \pm 0.04$	-0.87 ± 0.06	1.16
1−5	$+0.93 \pm 0.06$	-0.80 ± 0.04	1.16
0−2	$+0.79 \pm 0.05$	-0.85 ± 0.05	1.16
2−5	$+0.93 \pm 0.06$	-0.81 ± 0.05	1.17

ordinary quasars suggest that for the synchrotron emission, energy losses play the crucial part in the case when the source is tightly confined.

Our study established that the number of GPS galaxies decreases sharply with increasing redshift, starting from $z = 1$. We found neither GPS galaxies nor objects without optical counterparts in a rather large redshift interval from 1.8 to 4.5 (Fig. 3, 4). However, we found in this redshift interval a substantial number of quasars with no blazar properties (Fig. 5). The most distant GPS object in our sample is the galaxy J 1606+31 ($z = 4.56$, $\theta = 0.37$ mas). It is the only high-redshift GPS galaxy in the sample. The lack of distant GPS galaxies may also be due to the fact that, unlike brighter quasars, they were not found in the corresponding radio-source surveys because of their steep spectra. Possibly, the physical conditions of the ambient medium have to be studied at high and low redshifts.

We found differences between the spectral properties of GPS galaxies and quasars. Their common feature is a rather simple form of the radio spectrum. Unlike other compact extragalactic radio sources, they have no close-to-zero spectral indices. Spectral parts above and below the peak frequency for GPS sources are typically steep. The absorption mechanism in the optically thick emission region is not yet entirely understood. There is a general assumption that the low-frequency cut of the spectrum is due to synchrotron self absorption caused by the high density of the emitting electrons [27]. However, the free-free absorption has also been suggested to be able to produce the turnover at GHz frequencies as well as the peak frequency vs. size−anticorrelation observed in many of these sources [49]. Such a form of the radio spectrum can be described fairly well in terms of the model of synchrotron emission of an extragalactic radio source [23]. This model associates the convex form of the radio spectrum with the compactness, homogeneity of the structure and magnetic field. However, according to VLBI measurements, GPS objects have neither a homogeneous radio structure (see Table 1) nor a homogeneous magnetic field. Therefore observational data are somewhat inconsistent with theory and the parameters of the radio spectra never reach the computed values of $\alpha_{below} = +2.5$ and FWHM = 0.7 [2, 3].

There are statistically significant differences in the average values of α_{above} and FWHM between the subgroups galaxies and quasars of our sample. This result confirms the average spectral parameters found earlier based on the monitoring of a limited list of GPS sources at the RATAN-600 radio telescope [26]. The mean value of the γ index of the electron energy spectrum [23] is 0.4−0.5 higher for the galaxies (i.e. their energy spectra are steeper) than for the quasars [26].

Here γ is the exponent in the energy distribution $N(E) = KE^{-\gamma}$ of relativistic emitting electrons. This may be due both to the additional energy losses in galaxies [50] or to the possible presence of a flat-spectrum component in quasars. An analysis of this difference should become the subject of a separate study.

We find the low-frequency spectral index α_{below} to increase with z, and practically not to differ for galaxies and quasars. This may be due, e.g., to the increase of the ambient density with increasing redshift [8], lack of systematic measurements at low frequencies, or the use of non-simultaneous observational data.

The angular size of the emitting region in selected GPS candidates does not exceed 10 mas. At the same z the angular sizes of galaxies and quasars are on the same order of magnitude, whereas the luminosities of these objects may differ by one order of magnitude. Direct and indirect size estimates indicate that GPS quasars are more compact than GPS galaxies, suggesting the presence of a dense ambient medium. Note that because of the large redshifts of quasars the possible emission of their extended regions is below the detection limit for aperture synthesis systems [17].

Are GPS galaxies and quasars the same objects in terms of the Unified Scheme Models [51] scenario, or do their radio spectra just happen to have a similar form? The hypothesis that these are two different population types has been repeatedly discussed [11, 52]. Our results argue for the different physical nature of GPS galaxies and quasars. Within the framework of this study we formulated a number of specific problems, which require a separate investigation of GPS galaxies and quasars (the study of the physical conditions in circumnuclear regions, accretion rates, etc.), as well as modelling of synchrotron emission mechanisms in homogeneous objects with the given spectral parameters determined in this paper.

10. CONCLUSIONS

We compiled a new flux-density complete sample of GPS candidates (112 objects) based on an analysis of the data obtained with RATAN-600 and the available catalogs (CATS). A comprehensive study of these objects led us to the following conclusions:

We selected a total of 112 GPG candidates among the 467 objects with peaked spectra, which makes up about 2% of the entire sample of objects with fluxes $S_\nu \geq 200$ mJy at 4.8/5 GHz. Only 45 of the selected GPS candidates strictly satisfy the criteria for classical GPS. This amounts to about 1% of the entire sample, which is significantly less than expected: GPS objects are believed to constitute about one tenth of the bright extragalactic sources (at centimeter-wave frequencies).

Our analysis of the parameters of the radio spectra revealed that GPS galaxies have narrower spectra and higher high-frequency spectral indices than quasars. The low-frequency spectral index increases with redshift z and its values are comparable for the two types of objects.

The number of GPS galaxies in the sample decreases sharply with redshift, starting with $z = 1$. Galaxies and quasars have comparable angular sizes at the same z, whereas their luminosities may differ by one order of magnitude. We find a deficit of objects with low peak frequencies (several GHz) at large redshifts. It is possible that there are no objects with large synchrotron self-absorbing components at large z. Various indirect estimates confirm the presence of medium with high density of emitting particles in the circumnuclear regions of GPS objects.

The sample is substantially "contaminated" with FSRQs objects (Flat Spectrum Radio Quasars). As a result, the list of GPS objects includes blazars, which we plan to analyze more thoroughly because of the still unresolved problem of the GPS nature.

ACKNOWLEDGMENTS

REFERENCES

1. T. A. T. Spoelstra, A. R. Patnaik, and Gopal-Krishna, Astronom. and Astrophys. **152,** 38 (1985).
2. Ch. P. O'Dea, Publ. Astronom. Soc. Pacific **110,** 493 (1998).
3. Ch. P. O'Dea, S. A. Baum, and C. Stanghellini, Astrophys. J. **380,** 66 (1991).
4. Ch. P. O'Dea, Publ. Astronom. Soc. Pacific **110,** 493 (1998).
5. W. H. de Vries, P. D. Barthel, and Ch. P. O'Dea, Astronom. and Astrophys. **321,** 105 (1997).
6. I. Torniainen, M. Tornikoski, H. Terasranta, and M. F. Aller, Astronom. and Astrophys. **435,** 839 (2005).
7. Ch. P. O'Dea, C. Stanghellini, S. A. Baum, and S. Charlot, Astrophys. J. **470,** 806 (1996).
8. Ch. P. O'Dea, Monthly Notices Roy. Astronom. Soc. **245,** 20 (1990).
9. C. Stanghellini, Ch. P. O'Dea, D. Dallacasa, et al., Astronom. and Astrophys. Suppl. **131,** 303 (1998).
10. C. Stanghellini, Ch. P. O'Dea, S. A. Baum, et al., Astronom. and Astrophys. **325,** 943 (1997).
11. C. Stanghellini, D. Dallacasa, Ch. P. O'Dea, et al., Astronom. and Astrophys. **377,** 377 (2001).
12. R. B. Phillips and R. L. Mutel, Astronom. and Astrophys. **106,** 21 (1982).
13. A. G. Polatidis and J. E. Conway, Publ. Astronom. Soc. Australia **20,** 69 (2003).
14. C. Fanti, R. Fanti, D. Dallacasa, et al., Astronom. and Astrophys. **302,** 317 (1995).
15. A. C. S. Readhead, G. B. Taylor, W. Xu, et al., Astrophys. J. **460,** 612 (1996).
16. S. A. Baum, Ch. P. O'Dea, D. W. Murphy, and A. G. de Bruyn, Astronom. and Astrophys. **232,** 19 (1990).
17. C. Stanghellini, Publ. Astronom. Soc. Australia **20,** 118 (2003).
18. J. M. Bai and M. G. Lee, Jr. Korean Astron. Soc. **38,** 125 (2005).
19. J. A. Peacock and J. V. Wall, Monthly Notices Roy. Astronom. Soc. **198,** 843 (1982).
20. W. J. M. van Breugel, G. Miley, and T. Heckman, Astronom. J. **89,** 5 (1984).
21. C. Fanti, R. Fanti, P. Parma et al., Astronom. and Astrophys. **143,** 292 (1985).
22. D. Dallacasa, C. Stanghellini, M. Centonza, and R. Fanti, Astronom. and Astrophys. **363,** 887 (2000).
23. K. I. Kellermann and I. I. Pauliny-Toth, Annu. Rev. Astronom. Astrophys. **19,** 373 (1981).
24. M. G. Mingaliev, Yu. V. Sotnikova, M. G. Larionov, and A. K. Erkenov, Astronomy Reports **55,** 187 (2011).
25. M. Tornikoski, I. Torniainen, A. Lahteenmaki, et al., Astron. Nachr. **330,** 128 (2009).
26. M. G. Mingaliev, Yu. V. Sotnikova, I. Torniainen, et al., Astronom. and Astrophys. **544,** A25 (2012).
27. I. A. G. Snellen, R. T. Schilizzi, A. G. de Bruyn, et al., Astronom. and Astrophys. Suppl. **131,** 435 (1998).
28. O. V. Verkhodanov, S. A. Trushkin, and V. N. Chernenkov, Baltic Astronomy **6,** 275 (1997).
29. E. Massaro, P. Giommi, C. Leto, et al., Astronom. and Astrophys. **495,** 691 (2009).
30. M. Orienti, D. Dallacasa, S. Tinti, and C. Stanghellini, Astronom. and Astrophys. **450,** 959 (2006).
31. P. Augusto, J. I. Gonzalez-Serrano, I. Perez-Fournon, and P. N. Wilkinson, Monthly Notices Roy. Astronom. Soc. **368,** 1411 (2006).
32. S. Jeyakumar, D. J. Saikia, A. Pramesh Rao, and V. Balasubramanian, Astronom. and Astrophys. **362,** 27 (2000).
33. L. Xiang, D. Dallacasa, P. Cassaro, et al., Astronom. and Astrophys. **434,** 123 (2005).
34. A. L. Fey and P. Charlot, Astrophys. J. Suppl. **111,** 95 (1997).

35. L. Xiang, C. Reynolds, R. G. Strom, and D. Dalla-casa, Astronom. and Astrophys. **454,** 729 (2006).
36. D. Dallacasa, M. Bondi, W. Alef, and F. Mantovani, Astronom. and Astrophys. Suppl. **129,** 219 (1998).
37. N. E. Gugliucci, G. B. Taylor, A. B. Peck, and M. Giroletti, Astrophys. J. **622,** 136 (2005).
38. M. L. Lister, K. I. Kellermann, and I. I. K. Pauliny-Toth, in *Proc. 6th EVN Symp.*, Ed. by E. Ros, R. W. Porcas, A. P. Lobanov, and J. A. Zensus (2000), p. 135.
39. O. V. Verkhodanov, ASP Conf. Ser. **125,** 46 (1997).
40. M. F. Aller, H. D. Aller, and P. A. Hughes, Astronom. J. **399,** 16 (1992).
41. P. G. Edwards and S. J. Tingay, Astronom. J. **424,** 91 (2004).
42. R. L. Mutel, M. W. Hodges, and R. B. Phillips, Astronom. J. **290,** 86 (1985).
43. T. J. Pearson and A. C. S. Readhead, Astronom. J. **328,** 114 (1988).
44. D. Dallacasa, C. Fanti, R. Fanti, et al., Astronom. and Astrophys. **295,** 27 (1995).
45. R. Fanti, C. Fanti, R. T. Schilizzi, et al., Astronom. and Astrophys. **231,** 333 (1990).
46. Ch. P. O'Dea and S. A. Baum, Astronom. J. **113,** 148 (1997).
47. M. Tornikoski, I. Jussila, P. Johansson, et al., Astronom. J. **121,** 1306 (2001).
48. P. D. Barthel and G. K. Miley, Nature **333,** 319 (1988).
49. G. V. Bicknell, M. A. Dopita, and Ch. P. O'Dea, Astronom. J. **485,** 112 (1997).
50. N. S. Kardashev, Sov. Astron. **6,** 317 (1962).
51. C. M. Urry and P. Padovani, Publ. Astronom. Soc. Pacific **107,** 803 (1995).
52. I. A. G. Snellen, PhD Thesis (Univ. of Leiden, 1997).